Off-midplane launch of electron Bernstein waves for current drive in overdense plasmas

C. B. Forest[a] and P. K. Chattopadhyay
Department of Physics, University of Wisconsin, Madison, Wisconsin 53706

R. W. Harvey
CompX, Del Mar, California 92014

A. P. Smirnov
Moscow State University, Moscow, Russia

(Received 21 December 1999; accepted 14 February 2000)

Numerical modeling shows that localized, efficient current drive is possible in overdense toroidal plasmas (such as reversed field pinches and spherical tokamaks) using perpendicular launch of electron Bernstein waves. The wave directionality required for driving current can be obtained by launching the waves above or below the midplane of the torus and is a geometric effect related to the poloidal magnetic field. Wave absorption is strong, a result of the electrostatic nature of the waves, giving efficient suprathermal tail formation and current drive. © *2000 American Institute of Physics.* [S1070-664X(00)04405-0]

Prospects for magnetic fusion reactor concepts such as the spherical tokamak (ST)[1] and the reverse field pinch (RFP)[2] can be improved with the addition of localizable, high efficiency current drive. For the RFP, simulations have shown that the addition of localized noninductive current drive in the periphery of the profile can reduce the magnitude of the magnetic fluctuations responsible for its poor confinement.[3,4] The magnetic fluctuations in the RFP are due to resistive magnetohydrodynamic instabilities caused by current profile peaking; thus confinement in the RFP is ultimately the result of a misalignment between inductively driven current profiles and current profiles that are stable to tearing modes. If a technique such as rf current drive can be developed to noninductively sustain a Taylor-like state (defined here as a current profile linearly stable to all tearing modes), the confinement of the RFP and its potential as a reactor concept are likely to increase.

For the ST reactor to take advantage of its high stability and confinement prospects, a robust technique for noninductively ramping up and sustaining the current is needed; if this is done with the pressure generated bootstrap current, profile control using auxiliary current drive is still likely to be required for maintaining good magnetohydrodynamic stability. Additional current drive may also relax the stability requirements for a noninductively sustained ST by reducing the necessary bootstrap current.

Radio-frequency heating and current drive techniques developed on tokamaks and stellarators do not easily transfer to these low magnetic field, high density devices. The dielectric strength of RFP and ST plasmas (quantified by the ratio of the plasma frequency $\omega_{pe}^2 = n_e e^2/\epsilon_0 m_e$ to electron cyclotron frequency $\Omega_{ce} = eB/m_e$) is much larger than more conventional, high field tokamaks and stellarators: $\omega_{pe}/\Omega_{ce} > 5$ in present day RFPs and STs as illustrated in Fig. 1. This property imposes accessibility constraints on the minimum $N_\parallel$ ($N_\parallel > 7$ for present day RFPs and STs) for lower hybrid waves[5] which lowers the efficiency of current drive; it also leads to ion damping of high harmonic fast waves, reducing the power flow to electrons and therefore the current drive efficiency;[6,7] and finally, it renders current drive using electromagnetic waves in the electron cyclotron range of frequency impossible since both the ordinary and extraordinary modes are cut off. Although the lower hybrid waves and high harmonic fast waves can potentially be used for current drive, they may not be suitable for current profile control because of accessibility of ray trajectories, and because absorption profiles are sensitive functions of plasma parameters such as density and temperature.

This letter shows that the electron Bernstein wave (EBW) has potential for providing localized, highly efficient current drive in the RFP or ST. The EBW propagates at frequencies $\omega_{rf} \sim \Omega_{ce}$ when $\omega_{pe}/\Omega_{ce} > 1$, and is strongly absorbed near the cyclotron resonance. The potential of using the EBW for heating such overdense plasmas was recognized in the theoretical work of Preinhalter and Kopecky,[8,9] and recent experiments on the Wendelstein 7 advanced stellarator[10,11] have clearly demonstrated the feasibility; these studies have shown that obliquely launched O-mode electromagnetic radiation can efficiently couple power to EBWs through a double mode conversion process. An alternative coupling scenario based upon coupling of perpendicularly launched *X*-mode radiation[12,13] has also been studied. The EBW's potential for heating the ST[14,13] has already been noted, provided a suitable coupling technique can be developed. This letter does not address the coupling to the EBWs, rather it discusses only the propagation and absorption of the EBW.

The propagation and dispersion of the EBW is a complicated function of primarily magnetic field and electron temperature. Here, the propagation and absorption of the EBW is studied numerically using the Wentzel–Kramers–Brillouin approximation. The dispersion function used is a numerical

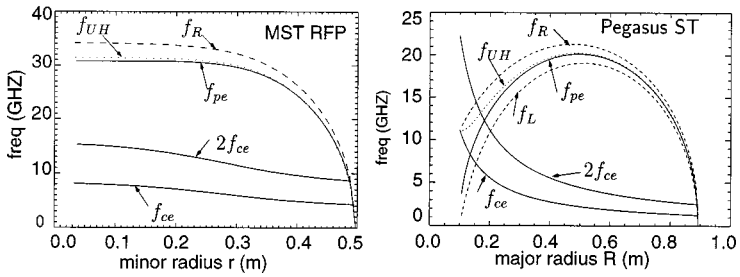

FIG. 1. Characteristic frequencies in the electron cyclotron range of frequencies on the MST (major radius 1.5 m, minor radius of 0.5 m reversed field pinch and the Pegasus ST ($R=0.4$ m, $R/a\approx 1.1$) experiments at the University of Wisconsin. The MST frequencies correspond to a 400 kA plasma current in MST, while the Pegasus equilibrium is a 300 kA plasma current discharge. $f_{L,R}$ are the right and left hand cutoff frequencies, f_{UH} is the upper hybrid frequency, $f_{\mathrm{ce}}=\Omega_{\mathrm{ce}}/2\pi$, and $f_{\mathrm{pe}}=\omega_{\mathrm{pe}}/2\pi$.

implementation of the fully electromagnetic, hot plasma dielectric tensor.[15] The determinant of the Hermitian part of the dielectric tensor results in a dispersion function $D[n_e(\mathbf{r}),B(\mathbf{r}),T_e(\mathbf{r}),N_\perp,N_\parallel,\omega]=0$. For a given density n_e, magnetic field strength B, temperature T_e, and $N_\parallel=ck_\parallel/\omega$ this equation can be solved to find $N_\perp$. The EBW dispersion is weakly sensitive to $N_\parallel$ and density, and can be qualitatively understood to satisfy $k_\perp\rho_e\sim O(1)$ between cyclotron harmonics; $k_\perp$ becomes large for frequencies just above cyclotron resonances, and $k_\perp$ vanishes (is cut off) when the wave frequency is slightly below a resonance.[15] Therefore D is predominantly a function of magnetic field and electron temperature.

Once a dispersion function D is known, the ray equations are[15]

$$\frac{d\mathbf{r}}{dt}=V_{g,\perp}\frac{\mathbf{N}-N_\parallel\mathbf{b}}{N_\perp}+V_{g,\parallel}\mathbf{b},\quad \frac{d\mathbf{N}}{dt}=\frac{c}{\omega}\frac{\partial D/\partial\mathbf{r}}{\partial D/\partial\omega},\tag{1}$$

where $\mathbf{b}$ is a unit vector aligned with the magnetic field, $\mathbf{N}=ck/\omega$, $N_\parallel=\mathbf{N}\cdot\mathbf{b}$, and

$$V_{g,\perp}=-\frac{c}{\omega}\frac{\partial D/\partial N_\perp}{\partial D/\partial\omega},\quad V_{g,\parallel}=-\frac{c}{\omega}\frac{\partial D/\partial N_\parallel}{\partial D/\partial\omega}.\tag{2}$$

The power absorption along a ray is related to the anti-Hermitian part of the dielectric tensor and requires special treatment to properly address the relativistic resonance condition.

The resonance absorption of EBW differs in several important ways from conventional electromagnetic wave absorption in the electron cyclotron range of frequencies. This is a result of the EBW having both $|N_\parallel|>1$ and $k_\perp\rho_e\gg 1$. The relativistic Doppler shifted cyclotron resonance condition,[16] which enters into the damping and rf quasilinear diffusion, is

$$\omega-k_\parallel v_\parallel-\frac{n\Omega_{\mathrm{ce}}}{\gamma}=0.\tag{3}$$

For EBWs with $|N_\parallel|>1$, the topology of the resonance in velocity space is a hyperbola. This implies that the resonance is both qualitatively and quantitatively different than for conventional electron cyclotron waves for which $|N_\parallel|<1$ and the resonance is an ellipse.

Absorption of ray energy can be calculated for each short section along the ray, i.e., ray element, using a calculation based on the quasilinear operator

$$p_{\mathrm{rf}}=\int d^3u(\gamma-1)mc^2\left.\frac{\partial f}{\partial t}\right|_{QL},\tag{4}$$

where $\partial f/\partial t|_{QL}$ models the quasilinear diffusion induced by the rf power. The lowest order electron distribution f is assumed to be axially symmetric in velocity space about the direction of the magnetic field. The fully relativistic quasilinear operator given by Stix[15] is used both for the damping Eq. (4) and for the calculation of the contribution to the quasilinear diffusion acting on the electrons due to each ray element: $\partial f/\partial t|_{QL}=\Sigma_{n=-\infty}^{n=\infty}(\partial/\partial\mathbf{u})\cdot\mathbf{D}\cdot(\partial/\partial\mathbf{u})f$,[15] with $\mathbf{u}=p/m_0$, and m_0=rest mass. The D_{uu} component of the QL operator is

$$D_{uu}=\frac{\pi e^2|E|^2}{2m^2\Delta k_\parallel}\left(\frac{|n_\parallel|}{c}\frac{1}{1-\dfrac{n\Omega_{\mathrm{ce}}}{\gamma\omega}}\right)\times\left|\cos\theta\frac{E_\parallel}{|E|}J_n+\sin\theta\left(\frac{E_+}{|E|}J_{n+1}\frac{E_-}{|E|}J_{n-1}\right)\right|^2.\tag{5}$$

The argument of the Bessel function J_n is $k_\perp u_\perp/\Omega_{\mathrm{ce}}$, and the θ is the pitch angle in momentum space. $|E|$ is the electric field amplitude for the field in the wave number range $\Delta k_\parallel$. This expression is evaluated along the resonance conic Eq. (3). The other tensor components of the QL tensor are simply related to Eq. (5). The values of $N_\parallel$, $k_\perp$, and the electric field polarizations in Eq. (5), the ''ray properties,'' are obtained from the dielectric tensor and dispersion relation at each point along the ray.

Since $k_\perp\rho_e\sim 1$, $\omega\sim\Omega_{\mathrm{ce}}$, the perpendicular phase velocity of the waves is $\sim v_{\mathrm{te}}$ and the full Bessel functions must be retained in Eq. (5) as well as in the dispersion relation. We have used the fully electromagnetic, hot (Maxwellian) dielectric tensor[15] for our calculation of ray trajectories and ''ray properties.'' Although the Hermitian part of the dielectric tensor is thereby nonrelativistic, the trajectories and ray properties depend primarily on the thermal part of the electron distribution function. In conjunction with the relativistic calculation of the damping in Eqs. (4) and (5), this will give an accurate model for conditions relevant to magnetic fusion, that is, for $T_e\ll mc^2$.

These aspects of EBW have been modeled with the combination of the GENRAY code[17] which calculates the EBW (among other) ray propagation paths, and the coupled CQL3D relativistic, Fokker–Planck bounce-averaged code[18] which calculates nonthermal bounce-averaged electron distributions in general noncircular toroidal devices as a function of $u_\parallel$,

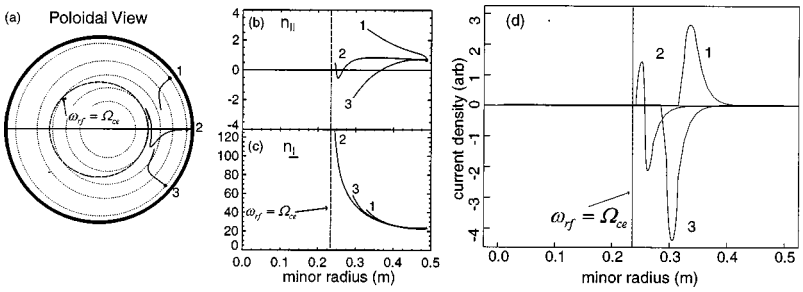

FIG. 2. (a) Ray trajectories for 8 GHz EBW rays in MST, launched in a 400 kA plasma, $T_e(0)=1$ keV, $n_e(0)=1.5\times10^{19}\,\mathrm{m}^{-3}$ representative of good confinement RFP plasmas. launched from three poloidal positions: $+40°$, $0°$, and $-40°$. The dotted lines are poloidal flux lines, the dashed line is the cyclotron resonance surface. The launched $N_\parallel=0.7$, corresponding to OXB coupling. Both the $N_\parallel$ (b) and $N_\perp$ (c) along the ray path for each set of rays. (d) The driven current density profile.

$u_\perp$, t and noncircular radial coordinate ρ. The distributions result from the velocity-space equilibrium of collisions and rf quasilinear diffusion due to the rf power. The ray energy is damped self consistently with the nonthermal electron distribution, by iteration between ray absorption and quasilinear diffusion.

These ray-tracing equations have been solved numerically for toroidally symmetric two-dimensional equilibria representing plasmas in the Madison symmetric torus (MST) reversed field pinch experiment[19] and the Pegasus spherical torus (ST) experiment.[20] Electron density and temperature profiles are representative of good confinement discharges in MST. For the purposes of this numerical study it was assumed that a technique for coupling to the EBWs exists; rays are initialized with $N_\perp$ and $N_\parallel$, which are on the EBW root of the dispersion function and then followed until a prescribed fraction of the energy is absorbed. For all calculations in this letter, the optical thickness $\tau=\int^s k_i ds \gg 1$; in practice, we only follow the EBW rays until $\tau\approx14$.

A representative ray tracing calculation for MST is shown in Fig. 2. Interestingly, for rays launched from the mid-plane the $N_\parallel$ of the wave undergoes oscillations about $N_\parallel=0$ as seen for ray (2) in Figs. 2(a) and 2(b). This $N_\parallel$ variation is disconcerting since it apparently destroys the directionality of the wave; the direction of the driven current is determined by the sign of $N_\parallel$ where the power is absorbed as seen in Fig. 2(d) where both co- and countercurrent are driven by ray (2). We have discovered that for EBW rays launched above and below the midplane, the $N_\parallel$ variation is unidirectional and determined by the poloidal launch position. Similar behavior has been found for ion Bernstein waves.[21,22] The shift depends upon whether the ray is launched in the upper or lower half of the torus; thus the directionality of the wave for current drive can be controlled and depends upon the side of the torus from which the wave is launched.

The $N_\parallel$ shift is a geometric effect resulting from variations of B within a flux surface, curvature, and magnetic shear. As such, it is strongly affected by the large poloidal field in RFPs and STs ($B_\theta/B\sim1$ in the edge of RFPs and STs). This can be understood from ray tracing Eq. (1) by evaluating the $N_\parallel$ evolution. Since density and temperature are constant on a flux surface and the equilibria is independent of toroidal angle,

$$\frac{dN_\parallel}{dt}=\mathrm{Sgn}(N_\parallel)\frac{c}{\omega}\frac{\partial B}{\partial s}\frac{\partial D/\partial B}{\partial D/\partial\omega}-\left(V_{g,\parallel}-\frac{N_\parallel}{N_\perp}V_{g,\perp}\right)\times\mathbf{N}\cdot(\hat{\mathbf{b}}\cdot\boldsymbol{\nabla})\hat{\mathbf{b}}-\frac{V_{g,\perp}}{N_\perp}\mathbf{N}\cdot(\mathbf{N}\cdot\boldsymbol{\nabla})\mathbf{b}. \tag{6}$$

Note, s represents the distance along the ray and each of the terms on the right hand side of Eq. (6) contribute to the $N_\parallel$ shift. The first term on the right hand side is due to variation of the magnetic field within a flux surface and is proportional to the strength of the poloidal field [for circular flux surfaces with (r,θ) representing minor radius and poloidal angle $(\partial B/\partial s)=(B_\theta/rB(\partial B/\partial\theta)]$. Several conclusions can be drawn regarding this term: if there is no variation of B within a flux surface, there is no up-shift; the direction of the upshift changes at the midplane [defined as the plane where variation in the vertical direction vanishes, i.e., $\partial B/\partial Z=0$]; and the rate of $N_\parallel$ upshift becomes larger as the wave approaches resonance [which is seen in Fig. 2(c), where $n_\perp$ grows]. Interestingly, for launch positions sufficiently close to the midplane the rays undergo oscillations in $N_\parallel$. The second term on the right hand side of Eq. (6) is related to curvature of the field, and the final term is related to the magnetic shear. All of these terms are exacerbated by the strong poloidal field in STs and RFPs.

The power deposition profile is determined by the location in the plasma at which Doppler shift cyclotron resonance occurs: $\Omega_{ce}(r)/\omega_{rf}\approx1-3N_\parallel(v_{ce}/c)$. Figure 2(d) shows that for low-$N_\parallel$ absorption (ray 2 launched from midplane) the Doppler shifted deposition is only several centermeters for MST parameters, however the large $N_\parallel$ values resulting from above and below midplane launch, the deposition can be located up to 10 cm further out. The width of the deposition profile, which is related to the thermal velocity spread, is also proportional to the $N_\parallel$ at the absorption location. For core current drive and heating, accessibility depends critically upon the equilibrium magnetic field. Waves which are resonant at the core may have to pass through a second harmonic resonance at the edge (see Fig. 1); the cyclotron damping of EBWs is strong at all harmonics and therefore the wave will not propagate beyond this point. The second harmonic overlap criteria imply that core heating of the RFP using EBWs will only be possible if $|B(a)|<2|B(0)|$.

Current drive calculations for Pegasus are shown in Fig. 3, for a situation representing perpendicular launch and an

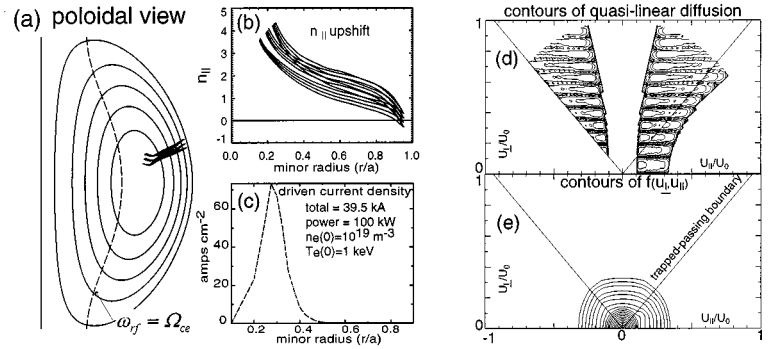

FIG. 3. (a) Current drive calculations for 2.8 GHz EBW launched in a 200 kA Pegasus discharge. The density and temperatures are taken to be the same as for the MST case above. The ray bundle is to represent an antenna spectrum of $\Delta N_{\|}=\pm 0.5$ with a launch position of $\theta=40°$. The dotted lines are surfaces of poloidal flux, the solid line labeled 1 is the position where $\omega_{ce}=\omega$. (b) The $N_{\|}$ evolution along each of the ray trajectories are shown. (c) The driven current density profile for 100 kW launched. (d) Contours of the quasilinear diffusion operator and (e) contours of the electron distribution function for the rays (U_0 is the electron velocity for a 300 keV electron and $v_{te}=0.03U_0$).

XB coupling scenario. A bundle of rays [seen in Figs 3(a) and 3(b)] is launched to represent the finite gain of a microwave antenna. The contours of the constant diffusion operator computed for this composite spectrum are shown for a flux surface in the region of strong absorption. The zeros of the Bessel function are seen in the quasilinear diffusion operator.

The contours of the modified distribution function show flattening of the distribution in the perpendicular velocity. The absorption is primarily at $v_{\|}\sim 3v_{te}$, which provides for relatively efficient current drive at this temperature. In this case, the current drive efficiency is $\eta_{CD}=I_{CD}n_eR_0/P_{rf}=0.15\times 10^{19}\,(\mathrm{A/m^2\,W})$, which is roughly a factor of three higher than measured in tokamak plasmas with comparable temperature and densities[23] and conventional fast wave current drive or electron cyclotron current drive. This is because the $N_{\|}$ upshift is larger ($N_{\|}>4$ in this region) and the absorption is stronger.

In summary, this letter has shown two things: (1) if the EBW can be launched, the wave directionality can be controlled by positioning of the antenna, and (2) the EBW absorption results in strong damping on tail electrons, which is needed for reliable current drive. In general, the $N_{\|}$ upshift resulting from the poloidal field and variations of B on a flux surface is much larger than the launched $N_{\|}$ of the wave and the driven current does not depend upon the details launching structure. In this case, the results presented here are germane to either OXB mode conversion, which is optimized for the obliquely launched, electromagnetic O mode, or to a tunneling of the wave via X-B, which is optimized for perpendicular launch angles. Interestingly, in the ST and RFP configurations, the mode conversion takes place very close to the edge of the plasmas, and the efficiency of mode conversion can be very high since the density scale lengths are short. Indeed several experiments are underway, which have already demonstrated the possibilities for heating via the EBW for both for the RFP and the ST, by observing emission from these plasmas. This letter has not attempted to evaluate the suitability of these waves for reactor-like plasmas, nor has it attempted to scale efficiencies to higher electron temperatures. Nonetheless, the conditions investigated in this letter will be applicable to edge current drive and current rampup, and therefore useful components of an ST reactor.

ACKNOWLEDGMENTS

The authors are grateful for helpful discussions with Abhay Ram, Stewart Prager, Ray Fonck, Ebo Uchimoto and Aaron Sontag. This work was supported by the U.S. Department of Energy.

[a]Electronic mail: cbforest@facstaff.wisc.edu

[1]Y.-K. M. Peng, D. J. Strickler, S. K. Borowski *et al.*, Fusion Technol. **8**, 338 (1985).
[2]H. Bodin and A. Newton, Nucl. Fusion **20**, 1255 (1980).
[3]C. Sovinec and S. Prager, Nucl. Fusion **39**, 777 (1999).
[4]E. Uchimoto, M. Cekic, R. W. Harvey, C. Litwin, S. C. Prager, J. S. Sarff, and C. R. Sovinec, Phys. Plasmas **1**, 3517 (1994).
[5]A. Bers, *Proceeding of the 3rd Topical Conference on Radio Frequency Plasma Heating*, Pasedena, CA, January 11–13 (California Institute of Technology, Pasedena, CA, 1978), p. A1-1.
[6]W. W. Heidbrink, E. D. Fredrickson, T. K. Mau, C. C. Petty, R. I. Pinsker, M. Porkolab, and B. W. Rice, Nucl. Fusion **39**, 1369 (1999).
[7]R. Majeskito Radio Frequency Power in Plasmas-Thirteenth Topical Conference, Annapolis, MD 1999 (to be published).
[8]J. Preinhaelter and V. Kopecký, J. Plasma Physics (1973).
[9]H. Weitzner and D. B. Batchelor, Phys. Fluids **22**, 1355 (1979).
[10]H. P. Laqua, V. Erckmann, and H. J. Hartfuß, Phys. Rev. Lett. **78**, 3467 (1997).
[11]H. P. Laqua, H. J. Hartfuß, and W7-AS Team, Phys. Rev. Lett. **81**, 2060 (1998).
[12]H. Sugai, Phys. Rev. Lett. **47**, 1899 (1981).
[13]A. K. Ram, A. Bers, and S. Schultz, Radio Frequency Power in Plasmas-Thirteenth Topical Conference, Annapolis, MD 1999.
[14]C. B. Forest, M. Ono, and G. Greene, Bull. Am. Phys. Soc. **35**, 2057.
[15]T. H. Stix, *Waves in Plasmas* (American Institute of Physics, New York, 1992).
[16]R. W. Harvey, M. C. McCoy, and G. D. Kerbel, Phys. Rev. Lett. **62**, 426 (1989).
[17]A. P. Smirnov and R. W. Harvey, Bull. Am. Phys. Soc. **40**, 1837 (1995).
[18]R. W. Harvey and M. G. McCoy, *Proceedings of IAEA Technical Committee Meeting on Advances in Simulation and Modeling of Thermonuclear Plasmas*, Montreal, Quebec (Inernational Atomic Energy Agency, Vienna, 1993), p. 489.
[19]R. Dexter, D. Kerst, T. Lovell, S. Prager, and J. Sprott, Fusion Technol., 131 (1991).
[20]R. Fonck and the Pegasus Team, Bull. Am. Phys. Soc. **44**, 267 (1999).
[21]M. Ono, Phys. Fluids B **5**, 241 (1993).
[22]A. Ram and A. Bers, Phys. Fluids B **3**, 1991 (1991).
[23]C. C. Petty, R. I. Pinsker, M. E. Austin *et al.*, Nucl. Fusion **35**, 773 (1995).